ESCRT regulates surface expression of the Kir2.1 potassium channel

Alexander R. Kolb[a,*], Patrick G. Needham[a,*], Cari Rothenberg[b], Christopher J. Guerriero[a], Paul A. Welling[b], and Jeffrey L. Brodsky[a]

[a]Department of Biological Sciences, University of Pittsburgh, Pittsburgh, PA 15261; [b]Department of Physiology, University of Maryland School of Medicine, Baltimore, MD 21201

ABSTRACT **Protein quality control (PQC) is required to ensure cellular health. PQC is recognized for targeting the destruction of defective polypeptides, whereas regulated protein degradation mechanisms modulate the concentration of specific proteins in concert with physiological demands. For example, ion channel levels are physiologically regulated within tight limits, but a system-wide approach to define which degradative systems are involved is lacking. We focus on the Kir2.1 potassium channel because altered Kir2.1 levels lead to human disease and Kir2.1 restores growth on low-potassium medium in yeast mutated for endogenous potassium channels. Using this system, first we find that Kir2.1 is targeted for endoplasmic reticulum–associated degradation (ERAD). Next a synthetic gene array identifies nonessential genes that negatively regulate Kir2.1. The most prominent gene family that emerges from this effort encodes members of endosomal sorting complex required for transport (ESCRT). ERAD and ESCRT also mediate Kir2.1 degradation in human cells, with ESCRT playing a more prominent role. Thus multiple proteolytic pathways control Kir2.1 levels at the plasma membrane.**

Monitoring Editor
Anne Spang
University of Basel

Received: Jul 17, 2013
Revised: Nov 6, 2013
Accepted: Nov 6, 2013

INTRODUCTION

Protein quality control (PQC) was initially described to reflect the fact that secreted proteins with various defects were unable to exit the endoplasmic reticulum (ER). Specifically, defects in protein glycosylation, folding, or assembly or protein aggregation led to ER retention (Hurtley and Helenius, 1989). More recently, it has become appreciated that PQC operates throughout the eukaryotic secretory pathway to ensure that toxic or misfolded proteins do not accumulate (Arvan *et al.*, 2002; Apaja *et al.*, 2010). In turn, regulated protein degradative systems provide a means to fine tune wild-type protein levels and thus their activities. Therefore even folded and functional proteins may be destroyed if existing levels are toxic or do not match cellular needs. If PQC or the regulated protein degradation system is defective or if the PQC machinery fails to recognize an aberrant protein, one of many human diseases may result (Gestwicki and Garza, 2012; Guerriero and Brodsky, 2012).

As noted, secretory pathway PQC begins in the ER, and proteins that fail to pass this step can be destroyed by ER-associated degradation (ERAD). ERAD substrates are first recognized by molecular chaperones and chaperone-like lectins, which target them for ubiquitination (Aebi *et al.*, 2010; Claessen *et al.*, 2012; Hebert and Molinari, 2012). During ubiquitination, ERAD substrates are retrotranslocated to the cytoplasm and delivered to and degraded by the 26S proteasome (Mehnert *et al.*, 2010; Smith *et al.*, 2011). If the ERAD machinery is overwhelmed or if aberrant proteins accumulate, the unfolded protein response is induced, and in some cases misfolded species can escape and advance to the Golgi. In these circumstances, ERAD substrates are returned to the ER (Vashist *et al.*, 2001; Haynes *et al.*, 2002; Taxis *et al.*, 2002), or in yeast a Golgi quality control system, which is absent in mammalian cells, recognizes and delivers substrates to the vacuole for degradation via the multivesicular body (MVB) pathway (Chang and Fink, 1995; Hong *et al.*, 1996; Spear and Ng, 2003; Wang and Ng, 2010; Coughlan *et al.*, 2004). PQC mechanisms also exist at the plasma membrane, and in

This article was published online ahead of print in MBoC in Press (http://www.molbiolcell.org/cgi/doi/10.1091/mbc.E13-07-0394) on November 13, 2013.

Address correspondence to: Jeffrey L. Brodsky (jbrodsky@pitt.edu).

*These authors contributed equally to this work.

Abbreviations used: CFTR, cystic fibrosis transmembrane conductance regulator; ERAD, endoplasmic reticulum–associated degradation; ESCRT, endosomal sorting complex required for transport; MVB, multivesicular body; PQC, protein quality control; SGA, synthetic gene array.

this case selected substrates are endocytosed and targeted to the lysosome (Huotari and Helenius, 2011). For example, the disease-associated ΔF508 mutant form of the cystic fibrosis transmembrane conductance regulator (CFTR) is an ERAD substrate but is also less stable than wild-type CFTR when delivered to the plasma membrane by low-temperature correction. Genome- and protein-wide screens revealed a significant number of factors required for the disposal of ΔF508 CFTR from the plasma membrane (Trzcinska-Daneluti *et al.*, 2009; Okiyoneda *et al.*, 2010), and for many substrates quality control at the plasma membrane also follows the MVB pathway (Jenness *et al.*, 1997; Arvan *et al.*, 2002; Apaja *et al.*, 2010; Keener and Babst, 2013; Zhao *et al.*, 2013). There are multiple mechanisms to ensure that unwanted secreted proteins are destroyed, but it is generally unclear how these systems cooperate and which pathway might be most important for the PQC of a given substrate.

To begin to investigate these questions, we reengineered and optimized a yeast expression system for the Kir2.1 potassium channel because relatively small changes in the amount of active, plasma membrane–resident Kir2.1 can be detected (Tang *et al.*, 1995; Nakamura and Gaber, 1998; Minor *et al.*, 1999). Like other inward-rectifying potassium channels, Kir2.1 is formed by the tetrameric assembly of identical subunits; each subunit has a potassium selectivity sequence, which is flanked by two transmembrane domains. The N- and C- termini form a large regulatory structure that surrounds the central pore (Schwalbe *et al.*, 2002). Tetrameric Kir2 potassium channels function primarily in heart, skeletal muscle, and neurons and consist of five family members—Kir2.1–2.4 and 2.6 (de Boer *et al.*, 2010; Hibino *et al.*, 2010). Kir2.1 is responsible for controlling membrane excitability in many cell types, especially in heart and skeletal muscle, and loss-of-function mutations in Kir2.1 result in Anderson–Tawil syndrome (ATS-1), a disorder characterized by periodic paralysis, long QT ventricular arrhythmias, and skeletomuscular dysplasia (Plaster *et al.*, 2001). Gain-of-function mutations in Kir2.1 lead to short QT syndrome, which can also cause cardiac arrhythmias (Priori *et al.*, 2005). These cases illustrate the importance of maintaining proper Kir2.1 levels. However, the factors necessary to support Kir2.1 trafficking and stability have not been explored in significant detail—hence our desire to identify these components using a systems-level approach.

We discovered that Kir2.1 in yeast traffics to the plasma membrane but resides predominately in the ER, where most of the protein is targeted for ERAD. Maximal Kir2.1 degradation required the AAA-ATPase Cdc48, the ER-associated E3 ubiquitin ligases Hrd1 and Doa10, and the cytoplasmic Hsp70 chaperone Ssa1. Because Kir2.1 supports the growth of *trk1*Δ*trk2*Δ yeast on low-potassium medium (Tang *et al.*, 1995; Nakamura and Gaber, 1998), this system also provided a unique opportunity to identify the spectrum of PQC and trafficking factors necessary to maintain active Kir2.1 at the plasma membrane. Of interest, ERAD-requiring factors were absent from the list of yeast mutants that significantly improved growth on low potassium, suggesting that the level of functional Kir2.1 is not regulated by ERAD. In contrast, most endosomal sorting complex required for transport (ESCRT) components were isolated. These data indicate that the plasma membrane and Golgi quality control systems regulate Kir2.1 residence at the plasma membrane. Consistent with this hypothesis, ESCRT also regulated Kir2.1 residence at the plasma membrane in human cultured cells. Together our results provide the first genomic analysis of the myriad degradative systems that operate on a single protein.

RESULTS

Kir2.1 is an ERAD substrate

The Kir2.1 potassium channel most likely encounters multiple PQC checkpoints as it travels through the secretory pathway to the plasma membrane. For example, an ATS-1 disease–causing mutation in the channel, Δ314-315, prevents channel trafficking from the Golgi apparatus to the plasma membrane by virtue of its inability to associate with the AP-1 clathrin-associated adaptor (Ma *et al.*, 2011). To gain a more comprehensive understanding of the Kir2.1 biosynthetic trafficking and degradation pathways, we refined a yeast expression system. To this end, a doubly tagged (myc and hemagglutinin [HA]) version of Kir2.1 was expressed under the control of a constitutive promoter. Analysis of Kir2.1 localization by indirect immunofluorescence microscopy primarily showed a perinuclear staining that colocalized with the ER-resident chaperone Kar2 (BiP; Figure 1A). Sucrose gradient centrifugation analysis indicated that a significant amount of Kir2.1 comigrated with Kar2 (Figure 1B, lanes 1–6). However, a fraction of Kir2.1 also comigrated with the plasma membrane protein Pma1 (lanes 9–11). These data suggest that whereas the majority of Kir2.1 is ER localized, a small pool advances to the plasma membrane. Thus the yeast expression system provides a model to explore PQC steps encountered by Kir2.1 as it travels through the secretory pathway.

Next the involvement of ERAD was assessed. For these studies, Kir2.1 stability was analyzed by cycloheximide chase in wild-type and mutant strains. We found that the channel was rapidly degraded, becoming almost undetectable within 90 min (Figure 2A). In *pdr5*Δ yeast, which allows studies with proteasome inhibitors, MG132 partially stabilized Kir2.1 from degradation (Figure 2A). Further, the AAA-ATPase, Cdc48, which extracts ERAD substrates from

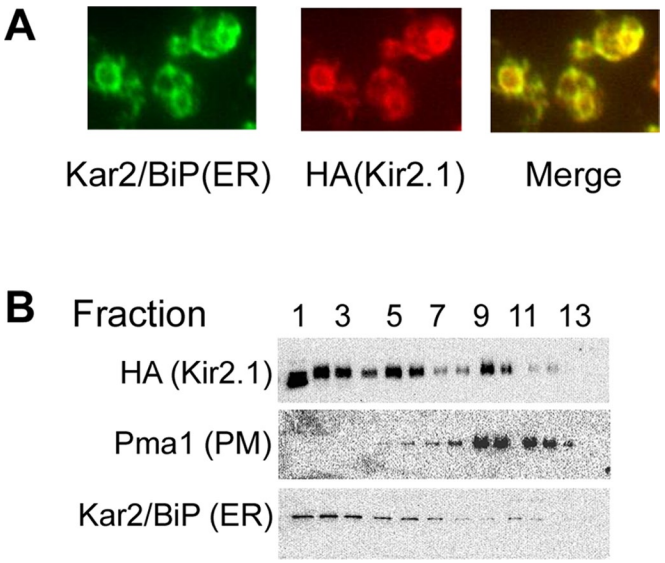

FIGURE 1: Kir2.1 resides primarily in the yeast ER. (A) Indirect immunofluorescence microscopy of yeast expressing Kir2.1. Fixed cells were probed with antibodies against the ER marker Kar2/BiP and the HA tag to visualize Kir2.1. Right, merge showing extensive colocalization. (B) Lysates from cells expressing Kir2.1 were analyzed by centrifugation in a 30–70% sucrose gradient under conditions to maximize ER and plasma membrane isolation (Roberg *et al.*, 1997). The gradient was fractionated from the top (fraction 1) to the bottom of the tubes (fraction 13). The migration of Kir2.1, the ER chaperone, Kar2/BiP, and the plasma membrane protein Pma1 were evaluated by Western blot analysis.

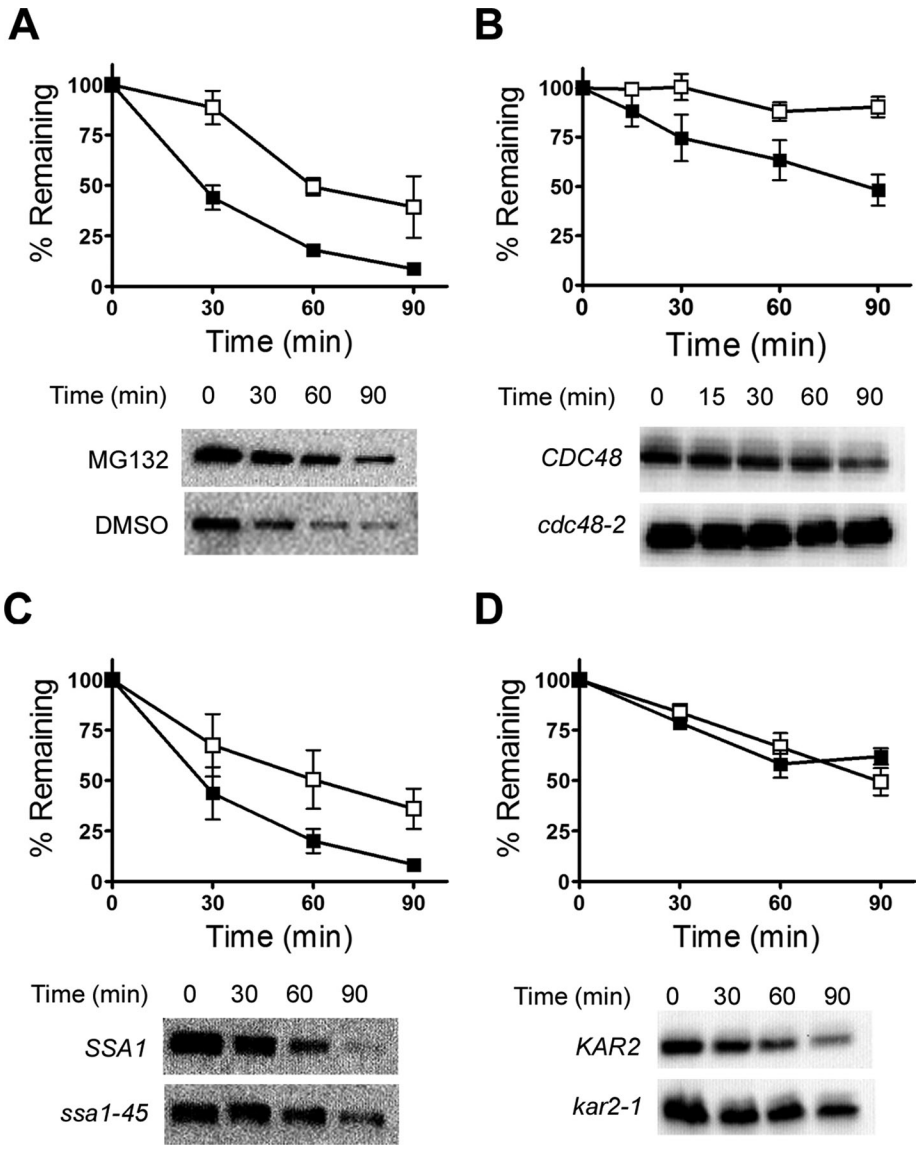

FIGURE 2: Kir2.1 degradation is proteasome and cytosolic chaperone dependent. Cycloheximide chase reactions were performed, and lysates were blotted with anti-HA antibody to measure Kir2.1 stability over time. (A) A *pdr5*Δ yeast strain was pretreated for 20 min with 100 μM MG-132 (□) or dimethylsulfoxide (■). Data represent means ± SE of three independent experiments. The degradation of Kir2.1 was also measured in (B) *CDC48* (■) or *cdc48-2* (□) mutant yeast, (C) *SSA1* (■) or *ssa1–45* (□) mutant yeast, and (D) *KAR2* ( ) or *kar2–1* (□) mutant yeast. Data represent means ± SE of four to six independent experiments. In each experiment, representative Western blots are shown at the bottom.

the ER membrane and into the cytosol (Wolf and Stolz, 2012), was required for degradation, since Kir2.1 was completely stabilized in a temperature-sensitive mutant, *cdc48-2*, at a nonpermissive temperature (Figure 2B). Combined with the data in Figure 1, these results establish Kir2.1 as an ERAD substrate in yeast.

To determine whether Hsp70 chaperones facilitate the ERAD of Kir2.1, we expressed the protein in the temperature-sensitive Ssa1 mutant *ssa1-45*. The cytosolic Hsp70, Ssa1, is required for the degradation of ERAD substrates with misfolded cytosolic domains (Hill and Cooper, 2000; Zhang *et al.*, 2001; Han *et al.*, 2007; Nakatsukasa *et al.*, 2008), and in line with these data, Kir2.1 degradation was attenuated at the nonpermissive temperature in the *ssa1-45* strain (Figure 2C). In contrast, Kir2.1 degradation was unaffected in a *kar2-1* mutant, which is required for the ERAD of substrates with misfolded lumenal domains (Plemper *et al.*, 1997; Brodsky *et al.*, 1999; Hill and Cooper, 2000; Figure 2D). These observations suggest that Kir2.1 folds poorly in yeast and is recognized as an ERAD substrate by the cytosolic Hsp70, Ssa1. As described later, Kir2.1 is also targeted for ERAD in mammalian cells.

Nearly all ERAD substrates in yeast are ubiquitinated by the E3 ligases Hrd1 and/or Doa10 (Claessen *et al.*, 2012). To investigate whether Kir2.1 was degraded in an Hrd1- and/or Doa10-dependent manner, we expressed Kir2.1 in *hrd1*Δ, *doa10*Δ, *hrd1*Δ*doa10*Δ, and *HRD1DOA10* strains. We found that Kir2.1 was stabilized to a similar level when either *HRD1* or *DOA10* was deleted, and when the genes encoding both E3s were absent, the protein was further stabilized (Figure 3A). We next asked whether deletion of the E3 ubiquitin ligases led to a decrease in Kir2.1 ubiquitination. Kir2.1 was immunoprecipitated from wild-type or *hrd1*Δ*doa10*Δ yeast and ubiquitin levels were examined by immunoblotting. As anticipated, deleting *HRD1* and *DOA10* led to ~40% reduction in Kir2.1 ubiquitination (Figure 3, B and C). Also as anticipated, an analysis of Kir2.1 residence by density centrifugation (see earlier discussion) in the *hrd1*Δ*doa10*Δ strain established that the protein accumulated primarily in the ER and to some extent in the Golgi; however, there was no significant increase in the plasma membrane pool, as defined by comigration with Pma1 (Supplemental Figure S1). Because Kir2.1 degradation is Ssa1 dependent (see earlier discussion), we anticipated the requirement for Doa10, which adds ubiquitin onto ERAD substrates with misfolded cytoplasmic domains, that is, ERAD-C substrates (Vashist and Ng, 2004; Carvalho *et al.*, 2006; Denic *et al.*, 2006). The more surprising Hrd1 dependence suggested that Kir2.1 folding defects are also recognized within the membrane (Sato *et al.*, 2009). Thus the Kir2.1 folding lesions in yeast are complex.

A yeast genomic screen identifies regulators of Kir2.1 biogenesis

To identify the spectrum of factors that affect Kir2.1 PQC, we performed a genomic screen. For these studies, we took advantage of the ability of Kir2.1 to rescue the growth of a yeast strain lacking the Trk1 and Trk2 potassium transporters (Tang *et al.*, 1995; Nakamura and Gaber, 1998). A synthetic gene array (SGA) query strain was engineered in which *TRK1* and *TRK2* were deleted and Kir2.1 was expressed. In low-potassium medium, growth of the strain correlates with Kir2.1 activity (Tang *et al.*, 1995; Nakamura and Gaber, 1998). Thus PQC factors can be identified in an SGA screen as mutants that enhance cell growth in a Kir2.1-dependent manner. We ultimately determined that expressing Kir2.1 from a *TEF* promoter on a centromeric plasmid (Supplemental Figure S2A) and then

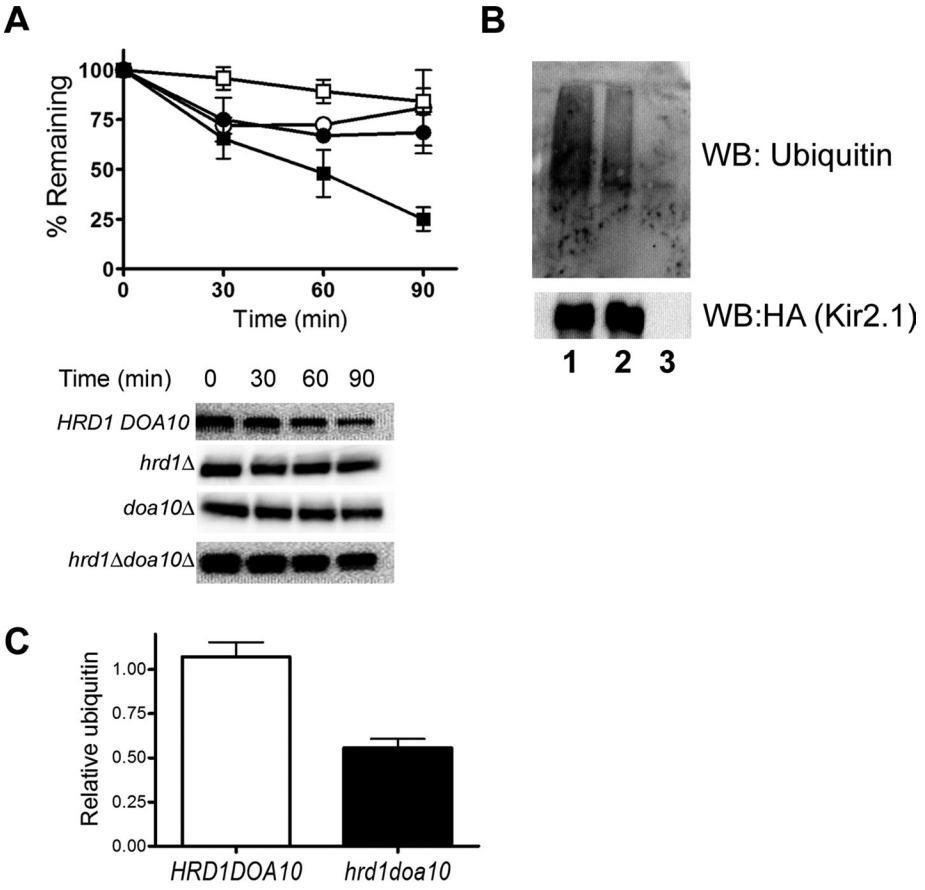

FIGURE 3: Kir2.1 degradation and ubiquitination are ubiquitin ligase dependent. (A) Cycloheximide chase reactions were performed, and lysates were blotted with anti-HA antibody to measure Kir2.1 stability over time in the following strains: wild type (■), *hrd1*Δ (●), *doa10*Δ (○), or *hrd1*Δ *doa10*Δ (□). Data represent means ± SE of four to six independent experiments. A representative Western blot from one experiment is shown below. (B) Kir2.1 expressed in either wild-type (lane 1) or *hrd1*Δ*doa10*Δ (lane 2) mutant yeast strains was immunoprecipitated from lysates with anti–HA-agarose beads, and Kir2.1 and conjugated ubiquitin were analyzed by Western blot analysis. The result from immunoprecipitation using cells containing a vector control is shown for comparison (lane 3). (C) Relative ubiquitination of Kir2.1 immunoprecipitated from wild-type and *hrd1*Δ*doa10*Δ yeast. The graph represents means ± SE from 13 precipitated samples of each strain, each from a distinct clone.

propagation on medium lacking potassium at pH 4 (Nakamura and Gaber, 1998) and 30°C (Supplemental Figure S2B) provided the optimal set of conditions to screen for genes that, when mutated, would augment growth on low potassium. As a control, we found that the residence of Kir2.1, as measured in sucrose gradient analyses as in Figure 1, was unaffected when cells were propagated at pH 4 (unpublished data).

Preventing the ERAD of some proteins increases their folding and secretion efficiencies (Qu *et al.*, 1996; Halaban *et al.*, 1997; Mitchell *et al.*, 1998; Schubert *et al.*, 1998; Vij *et al.*, 2006; Kincaid and Cooper, 2007; Grove *et al.*, 2009; Fisher *et al.*, 2011). Consistent with Kir2.1 perhaps behaving in a similar manner, deletion of *DOA10* subtly increased growth of the *trk1*Δ*trk2*Δ strain on low potassium when Kir2.1 was expressed (Supplemental Figure S3).

Having established that the system may detect PQC factors for Kir2.1, we conducted a genomic screen. First, the query strain was crossed to the yeast deletion collection using established SGA methodology (Tong and Boone, 2006). Next the resulting haploid strains, which each lacked one of 4848 nonessential yeast genes, were screened on selective medium at pH 4 in the absence of added potassium ([K^+] < 10 mM; Nakamura and Gaber, 1998). A total of 271 strains that exhibited significantly increased growth on low potassium were identified (see Figure 4A for one example). To focus our efforts, we eliminated 36 strains with mutated genes that compromised select biosynthetic pathways or represented characterized transcription and translation factors. In addition, 20 strains containing dubious open reading frames were not considered further.

Fresh isolates of the remaining 215 strains were crossed to the query strain containing either a vector control or the Kir2.1 expression vector and rescreened under a higher level of stringency to eliminate possible false positives. Added into this analysis were strains lacking genes that encode members of protein complexes (e.g., ESCRT; see later discussion) that featured prominently in the preliminary screen. The 95 strongest hits from this second-round screen were selected and ranked by measuring growth in liquid culture in 96-well plates. The ratio of the doubling time of a vector-only control strain to the same strain expressing Kir2.1 was calculated to produce a growth score. The analysis identified 54 deletion strains that reproducibly increased growth in a Kir2.1-dependent manner, each having a significantly higher growth score than the query strain containing the vector-only control (Figure 4B, Table 1, and Supplemental Table S1). To our surprise, genes required for ERAD were completely absent from this list, suggesting that the modest increase in growth when *DOA10* was deleted (Supplemental Figure S2) was below our cutoff. Instead, nearly all of the identified genes are associated with secretory pathway function at or beyond the Golgi. For example, a member of the phosphatidylinositol 3-kinase complex (Vps38) that regulates carboxypeptidase Y (CPY) sorting and interacts with the retromer complex represented the strongest hit (Kihara *et al.*, 2001; Burda *et al.*, 2002). Also prominent among the hits were a large number of ESCRT proteins (Did2, Vps36, Vps27, Vps22, Vps2, Vps23, Vps37, Mvb12, and Vta1).

ESCRT is involved in Golgi and plasma membrane quality control (Li *et al.*, 1999; Reggiori and Pelham, 2002; Apaja *et al.*, 2010; Okiyoneda *et al.*, 2010; Wang *et al.*, 2011), so we directly examined the role of select ESCRT members in Kir2.1 protein biogenesis. First, a *VPS23*-null strain (*vps23Δ)* strain, which also lacked *TRK1* and *TRK2,* was constructed, and after introduction of the Kir2.1 expression vector, the yeast were rescreened on low-potassium medium. Improved growth by Kir2.1 in the *trk1*Δ*trk2*Δ*vps23*Δ strain was quite prominent but was significantly decreased in a *trk1*Δ*trk2*Δ*VPS23* background (Figure 5A). To confirm that rescue on low-potassium medium was associated with Kir2.1 activity, we created a well-characterized loss-of-function mutation in Kir2.1, replacing the potassium selectivity filter ^{144}GYG^{146} sequence with ^{144}AAA^{146} (Tinker *et al.*, 1996). After the expression plasmid was introduced into cells, the inactive channel was unable to rescue growth, even though it

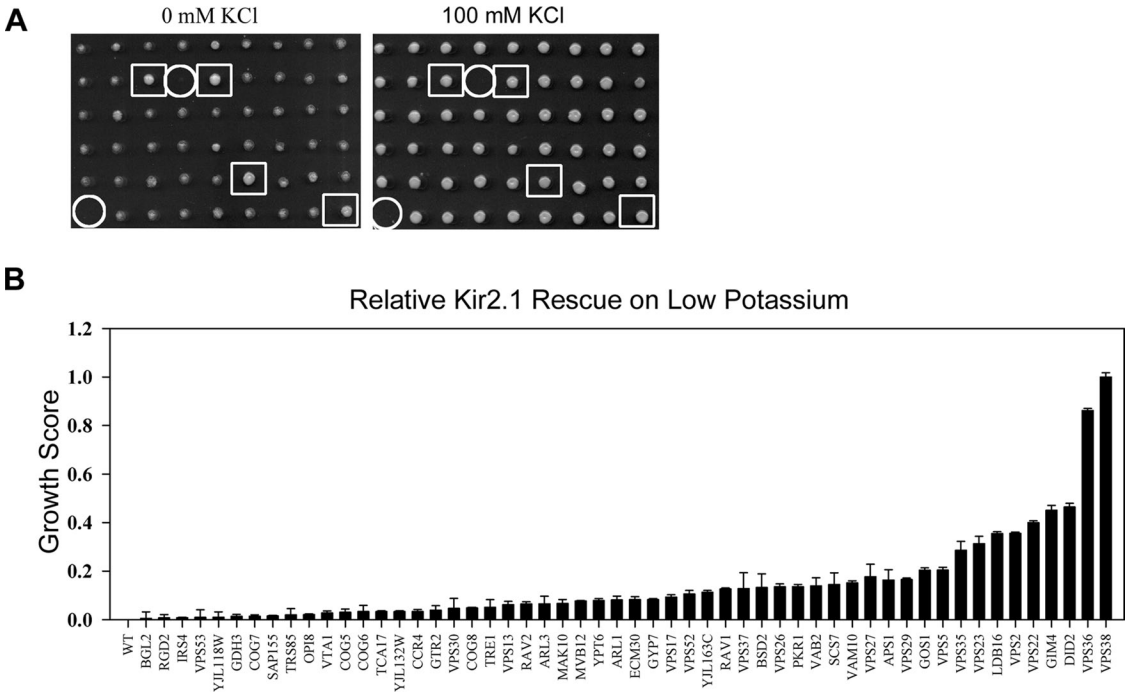

FIGURE 4: A genetic screen identifies ESCRT as a major effector of Kir2.1 plasma membrane residence. (A) Representative section of a plate after the mating of a query strain expressing Kir2.1 to the yeast deletion collection. Haploid progeny were plated on selective medium with either 0 or 100 mM KCl, as indicated. Medium containing 100 mM KCl serves as a control for equal growth among the different mutant strains. Circles represent negative controls in which a strain was absent and used as a plate identifier. Boxes represent strains that showed significantly increased growth compared with average colony growth on the plate at 0 mM K^+. (B) The Kir2.1 growth score of each hit was calculated based on the doubling time of the strains with an empty vector control divided by the doubling time of strains expressing the Kir2.1 expression vector. The medium contained a final concentration of 2.5 mM K^+. The growth score values were then normalized to *vps38*Δ, which was the strongest hit. All strains are deleted for *TRK1* and *TRK2,* as well as the indicated gene. Error bars SD of three independent measurements.

was expressed at similar levels as wild-type Kir2.1 (Figure 5, A and B). To ensure that Kir2.1-mediated rescue was unaffected by the presence of embedded epitopes, we expressed an untagged form of Kir2.1 in *trk1*Δ*trk2*Δ cells that restored growth on low-potassium medium to a similar extent as that observed for the doubly tagged Kir2.1 construct (Supplemental Figure S4).

A disease-associated mutation triggers the ERAD of Kir2.1

To test whether a disease-causing trafficking mutation makes the channel susceptible to PQC at an early point in the secretory pathway, we introduced the ATS-1 mutation Δ314-315, which blocks Golgi export (Ma *et al.*, 2011). As expected, the mutant failed to rescue growth of *trk1*Δ*trk2*Δ yeast on low potassium. Because the Δ314-315 mutant protein was expressed at significantly lower levels than wild-type Kir2.1 (Figure 5, A and B), we then assessed whether the mutation targets the channel for proteasomal- or vacuolar-dependent degradation. MG132 stabilized Kir2.1Δ314-315 in the *pdr5*Δ yeast strain, but degradation was unaffected when vacuolar proteases were inactivated (Supplemental Figure S5). These results reflect other observations that Kir2.1Δ314-315 is stabilized when the proteasome is inhibited in HeLa cells (unpublished data; see later discussion). Together the data suggest either that defects in the progression of the Andersen–Tawil mutant protein beyond the Golgi result in retrieval to the ER and proteasomal degradation, or the protein exhibits an ER folding defect as well as a defect in AP1-mediated trafficking.

Proteasome- and ESCRT-dependent degradation of Kir2.1 in human cells

The results presented in the preceding sections indicate that Kir2.1 is an ERAD substrate in yeast but that later steps in the secretory pathway play a more profound role in controlling the population of active Kir2.1 at the plasma membrane. To examine whether these phenomena were evident in mammalian cells, we examined Kir2.1 stability in HeLa cells.

Cycloheximide chase analysis confirmed that Kir2.1 was degraded by the 26S proteasome, as it was in yeast, although to a lesser extent (Figure 6, A and B). Because the majority of wild-type Kir2.1 turnover was proteasome independent, we next examined whether Kir2.1 was degraded in the lysosome. Consistent with a role for lysosomal degradation in controlling Kir2.1 levels, leupeptin increased Kir2.1 steady-state levels, as reported (Jansen *et al.*, 2008; Nalos *et al.*, 2011; Figure 6, C and D). Further, leupeptin addition augmented colocalization with a late endosomal/lysosomal marker, CD63 (Figure 6E). In metabolic pulse-chase experiments, treatment with leupeptin again stabilized Kir2.1 in HeLa cells (Supplemental Figure S6) and, as anticipated, MG132 addition led to more modest effects (unpublished data).

To determine whether ESCRT was required for the lysosome dependent degradation of Kir2.1, we depleted the ESCRT components Tsg101 (an ESCRT-I component that is the yeast Vps23 homologue; Rothman and Stevens, 1986; Robinson *et al.*, 1988; Babst *et al.*, 2000) and HRS (an ESCRT-0 component that is a homologue

Family	Function	Genes				
		Protein-trafficking complexes				
ESCRT and ESCRT partners	Formation of MVBs	Vps23	Vps37	Mvb12	Vps22	Vps36
		Vps2	Did2	Vta1	Opi8	Vps27
PI3K II	PI3 kinase involved in vacuolar protein sorting	Vps38	Vps30			
Retromer	Retrieval of vacuolar-targeted proteins	Vps5	Vps17	Vps26	Vps29	Vps35
GARP	Retrieval of vacuolar-targeted proteins	Vps52	Vps54			
TRAPP	Golgi trafficking	Tca17	Trs85			
COG	Golgi cytosolic tethering complex	Cog5	Cog6	Cog7	Cog8	
RAVE	Endosomal trafficking, Golgi localization, V-ATPase assembly	Rav1	Rav2			
AP-1	Clathrin adapter protein complex associated with protein sorting at the Golgi	Aps1				
BLOC	Endosomal sorting	Vab2				
EGO and GSE	Vacuolar invagination	Gtr2				
		GTPase and associated proteins				
GTPase	Regulates trafficking through GTP hydrolysis	Arl1	Ypt6	Arl3		
GAP	Stimulates GTPase activity	Gyp7	Rgd2			
Rsp5 adaptors	Facilitate ubiquitination by the Rsp5 ubiquitin ligase	Bsd2	Tre1			
		Vacuole function				
Morphogenesis	Vacuolar fusion	Vam10				
Assembly factors	V-ATPase assembly	Pkr1				
Phosphatase activators	Stimulate dephosphorylation	Sap155	Irs4			
		Other				
v-SNARE	Mediates vesicle fusion	Gos1				
Prefoldin complex	Transfers proteins to chaperonin	Gim4				
Glutamate dehydrogenase	Synthesizes glutamate	Gdh3				
Sphingolipid α-hydroxylase	Long-chain fatty acid biogenesis	Scs7				
NatC	Protein acetylation	Mak10				
CCR4-NOT	Transcription regulation	Ccr4				
Endo-β-1,3-glucanase	Cell wall maintenance	Bgl2				
Uncharacterized	Ldb16	Vps13	Ecm30	YJL132w		
		YJL118w	YJL163c			

BLOC, biogenesis of lysosome-related organelle complex-1; CCR4-NOT, carbon catabolite repression 4-negative on TATA; EGO, exit from rapamycin-induced growth arrest; GSE, Gap1p sorting in the endosomes; NatC, N-terminal acetyltransferase C; RAVE, regulator of the (H+)-ATPase of the vacuolar and endosomal membranes; v-SNARE, vesicle soluble *N*-ethylmaleimide–sensitive factor attachment protein receptor.

TABLE 1: Genes that, when deleted, increase the growth of *trk1*Δ*trk2*Δ yeast on low potassium.

of yeast Vps27; Robinson *et al.*, 1988; Komada *et al.*, 1997; Bilodeau *et al.*, 2002). Treatments with targeted small interfering RNAs (siRNAs) led to nearly complete absence of Tsg101 and ~50% decrease in the amount of HRS (Figure 6, F and G). In parallel, there was a corresponding increase in Kir2.1 abundance (Figure 6H). Addition of leupeptin did not lead to a further increase in Kir2.1 when the ESCRT components were knocked down, consistent with delivery to and degradation of the channel in the lysosome (Figure 6I). Our collective data from the yeast and human cell models demonstrate that ESCRT-dependent targeting of Kir2.1 to the vacuole/lysosome regulates the levels of Kir2.1 at the plasma membrane. These results are also the first to implicate ESCRT in the regulation of a Kir potassium channel.

DISCUSSION

We demonstrated that Kir2.1 is subject to PQC at multiple levels in both yeast and human cells. An initial characterization of Kir2.1 in yeast revealed a majority of the channel residing in the ER,

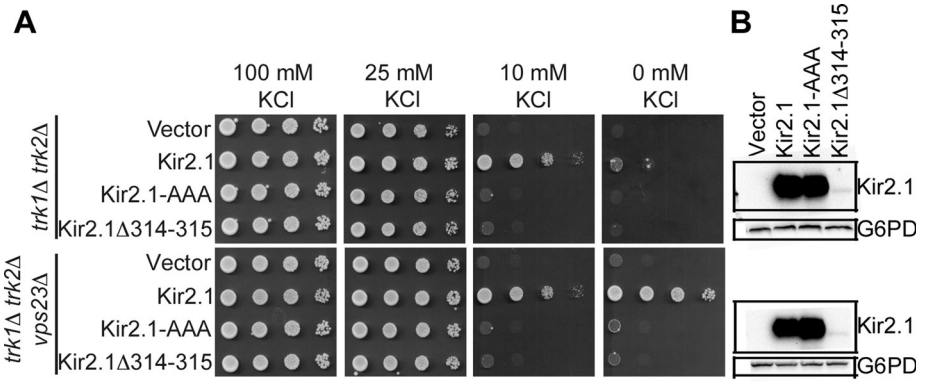

FIGURE 5: Deletion of *VPS23* increases Kir2.1-dependent rescue of *trk1*Δ*trk2*Δ on low potassium. (A) The vector control or the indicated plasmids were introduced into the query strain (*trk1*Δ*trk2*Δ) and into a *trk1*Δ*trk2*Δ*vps23*Δ strain. Tenfold serial dilutions were plated onto selective medium with 100, 25, 10, or 0 mM KCl, and growth was measured after 2 d at 30°C. (B) Equal numbers of cells were collected from the plates, lysed, and analyzed by SDS–PAGE and blotted with anti-HA antibody to assess Kir2.1 levels. G6PD served as a loading control.

where it is targeted for ERAD. In contrast, our genomic screen revealed that the abundance of active Kir2.1 at the plasma membrane is controlled by vacuolar targeting factors. These data suggest that a larger, permanently misfolded population of Kir2.1 is delivered to the ERAD pathway, which may be unable to mature or become active. By contrast, the pool of Kir2.1 that migrates beyond the ER appears to be in a folding-competent state, in which it is regulated by ESCRT and associated factors (see later discussion). In one model, this population may transiently adopt misfolded conformations, and defects in ESCRT-mediated degradation could then rescue this protein pool so it functions at the plasma membrane. The notion of an unstable population of maturing and even functional ion transporters is not new (Hill and Cooper, 2000; Helliwell *et al.*, 2001; Lu *et al.*, 2007; Apaja *et al.*, 2010), but our data represent the first hint of the relative strengths of unique quality control mechanisms that may act on a single protein in the secretory pathway.

To some extent the studies in HeLa cells validated the use of yeast as a model to identify the pathways that affect Kir2.1 biogenesis. Kir2.1 is regulated by both ERAD and ESCRT-mediated lysosomal degradation, as in yeast, but the relative contribution of each is inverted. In yeast, the majority of Kir2.1 was degraded by ERAD, with a minor Kir2.1 population being targeted to the vacuole. Based on our calculations, rescue of *trk1*Δ*trk2*Δ yeast growth requires very few active Kir2.1 channels on the surface, so the screen provides a sensitive method to detect this minor pool. Nevertheless, rapid ERAD-mediated turnover precluded our ability to reproducibly measure changes in Kir2.1 organellar residence in the mutant strains (unpublished data). In contrast, Kir2.1 is primarily degraded in the lysosome in HeLa cells, whereas a smaller population of Kir2.1 is targeted for ERAD, and based on this fact, significant changes in the intraorganellar pool were evident (Figure 6).

One explanation for the relative instability of Kir2.1 in yeast may be unique lipid compositions. Lipids such as cholesterol and phosphatidylinositol 4,5-bisphosphate (PI-4,5-bisP) alter Kir2.1 function and may influence its stability (Huang *et al.*, 1998; Romanenko *et al.*, 2004). Yeast lack cholesterol (but contain ergosterol), and the levels of PI-4,5-bisP might differ significantly between yeast and human cells. In addition, yeast could lack a Kir2.1 cofactor, which stabilizes the protein. For example, a yeast screen was used to identify cofactors for a rodent monocarboxylate transporter that increased transporter levels and function (Makuc *et al.*, 2004). It is unknown whether a Kir2.1 cofactor exists in mammals, but a yeast-based screen provides a route to identify this putative factor, as well as intragenic mutations that affect Kir2.1 function and PQC.

Numerous ESCRT components were identified in the screen (Table 1 and Supplemental Table S1). Substrate selection in the MVB pathway begins with the recognition and clustering of ubiquitinated cargo by ESCRT-0 (e.g., Vps27, which was identified in the screen; Bilodeau *et al.*, 2002; Wollert and Hurley, 2010; Mayers *et al.*, 2011). ESCRT-I (Vps23, Vps37, and Mvb12 were represented in the screen) and ESCRT-II (Vps22 and Vps36 were isolated) are then recruited and confine cargo at the site of vesicle formation, which initiates vesicle invagination before ESCRT-III (e.g., Vps2, Table 1) is recruited (Teo *et al.*, 2004, 2006; Gill *et al.*, 2007; Kostelansky *et al.*, 2007; Wollert and Hurley, 2010). Association of ESCRT-III leads to cargo deubiquitination (McCullough *et al.*, 2006) and vesicle maturation (Wollert *et al.*, 2009; Wollert and Hurley, 2010). In yeast the Vps4–Vta1 complex (Vta1, Table 1) then aids in disassembly of the ESCRT complex to complete vesicle formation (Babst *et al.*, 1998; Azmi *et al.*, 2008).

We also identified other factors that regulate Golgi trafficking and vacuolar function (Table 1). Deletion of *VPS38*, which encodes a component of phosphatidylinositol 3-kinase complex II (PI3KII), most strongly affected Kir2.1-dependent rescue. PI3K is a member of two complexes, PI3KI and PI3KII. PI3KI localizes primarily to the vacuole and is involved in autophagy, whereas PI3KII resides in the Golgi and endosome and regulates protein trafficking from the endosome to the Golgi (Burda *et al.*, 2002; Obara *et al.*, 2006). Deletion of the genes encoding Vps38 and another component of the PI3K complexes, Vps30, compromises retromer activity (Burda *et al.*, 2002). Retromer functions in the recovery of proteins from the endosome to the Golgi (Seaman *et al.*, 1998), and all five members of the retromer complex (Vps5, Vps17, Vps26, Vps29, and Vps35) are represented within the 20 strongest hits in the screen. Although the mechanism is undefined, deletion of retromer increases plasma membrane residence of other membrane proteins in yeast, flies, and worms (Kim *et al.*, 2007; Korolchuk *et al.*, 2007; Dang *et al.*, 2011). More recently, the receptor activator of NF-κB (RANK), which is involved in osteoclast formation, was shown to be inhibited by retromer-mediated transport from the endosome to the Golgi, thereby increasing RANK at the plasma membrane in murine osteoclasts (Xia *et al.*, 2013). Inhibition of retromer may cause a factor that would normally antagonize Kir2.1 plasma membrane residence, such as a Golgi retention factor, to be degraded, or retromer may aid in retrieving a population of Kir2.1 that traffics through an endosomal intermediate en route to the plasma membrane.

Additional proteins that regulate the trafficking/localization of proteins at the Golgi and endosome were identified as weaker hits. These include Golgi-associated GTPases (Arl1, Arl3, Ypt6) that regulate Golgi–endosome trafficking (Li and Warner, 1996; Luo and Chang, 1997; Behnia *et al.*, 2004). Ypt6 interacts with Vps52 in the Golgi-associated retrograde protein (GARP) complex, which retrieves proteins from the endosome to the Golgi; two GARP components were among the hits (Vps52 and Vps53; Conibear and Stevens, 2000; Siniossoglou and Pelham, 2002). Other protein

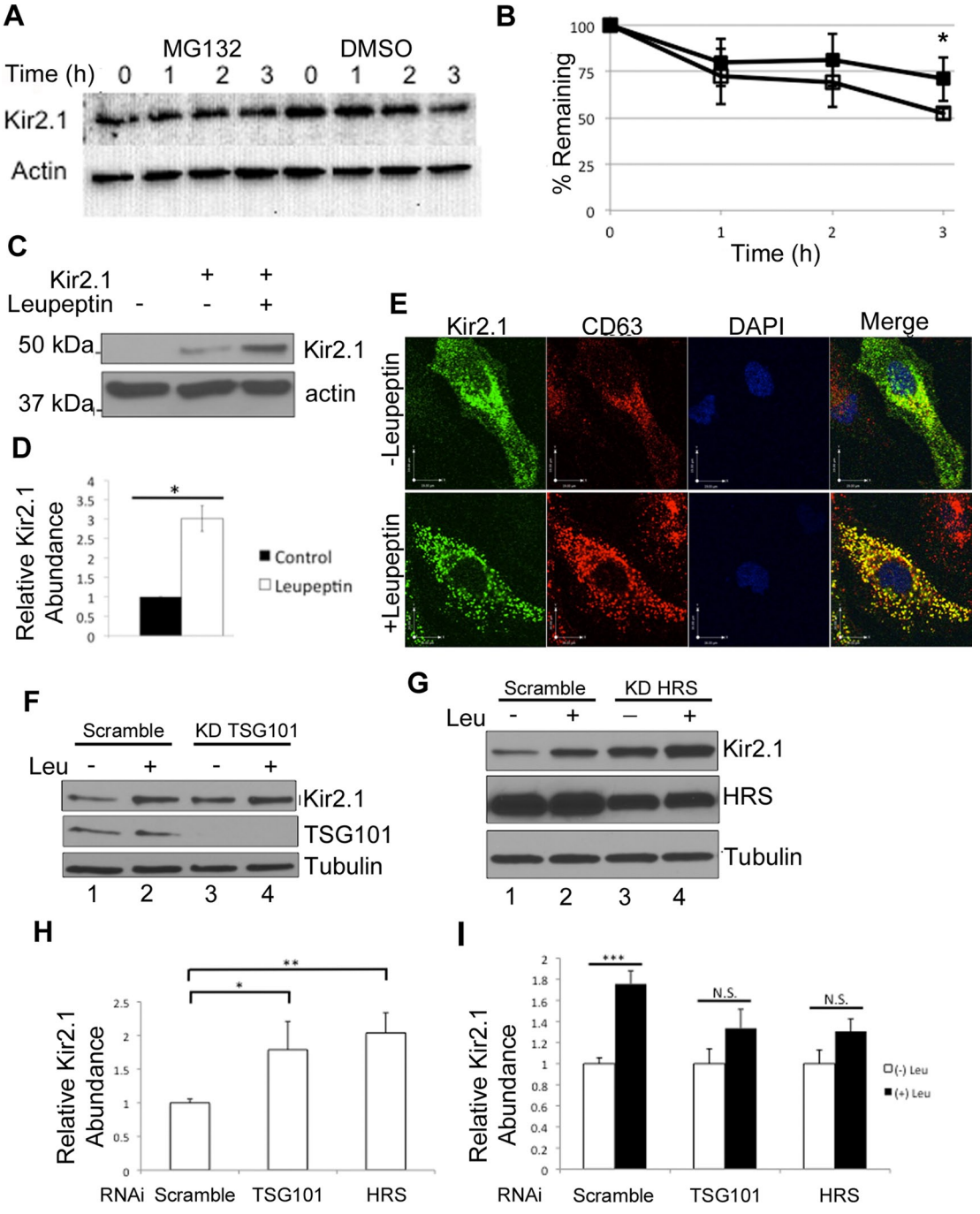

FIGURE 6: Kir2.1 degradation is primarily lysosomal dependent and requires ESCRT. (A, B) Kir2.1 stability was analyzed by a cycloheximide chase in HeLa cells. HeLa cells transfected with pcDNA3.1-HA-Kir2.1 were treated with 15 μM MG132 (□) or dimethylsulfoxide (■) and harvested, lysed, and analyzed by SDS–PAGE. Kir2.1 was detected with an anti-HA antibody. Actin levels served as a loading control. (A) A representative blot. (B) Data represent means of four or five experiments ± SD. (C) HeLa cells transfected with HA-Kir2.1 were treated with 100 μM leupeptin for 18 h. Cells were then lysed and visualized by Western blot. (D) Means ± SE from three independent trials from part C treated with (□) or without (■) leupeptin. (E) Confocal microscopy was performed in HeLa cells transfected with pcDNA3.1-HA- Kir2.1. Cells were treated with 100 μM leupeptin as described in *Materials and Methods* and were mounted in medium containing DAPI. Merge, colocalization of Kir2.1 (green) and CD63 (red), a marker of endosomes/lysosomes (yellow). (F–I) HeLa cells were cotransfected with the indicated siRNA and pcDNA3.1-HA-Kir2.1, and after 72 h, cells were harvested and the levels of Kir2.1, TSG101, HRS, and tubulin measured. Where indicated, 100 μM leupeptin was added to cells for 18 h. Tubulin served as a loading control. (H) The levels of Kir2.1 when TSG101 or HRS were knocked down (lane 3 from F and G) were normalized to the scramble control (lane 1 from F and G) to determine the effect of siRNA on Kir2.1 abundance. The data represent means ± SE of six to eight independent trials. (I) Levels of Kir2.1 in the presence of leupeptin when TSG101, HRS, (lane 4 from F and G), or scramble (lane 2 from F and G; solid bars) siRNAs were transfected and normalized to Kir2.1 levels when leupeptin was absent (lanes 1 and 3; open bars) to determine the magnitude of the leupeptin response. The data represent means ± SE of six to eight independent trials. *$p < 0.05$, **$p < 0.01$, ***$p < 0.001$.

complexes involved in trafficking within the Golgi, such as the TRAPP complex (Tca17, Trs85; Sacher *et al.*, 2000; Montpetit and Conibear, 2009) and the conserved oligomeric Golgi (COG) complex (Cog5, Cog6, Cog7, Cog8; Ram *et al.*, 2002; Ungar *et al.*, 2002), were among the 18 weakest hits, but whether these play a direct or indirect role in Kir2.1 trafficking is unclear. Nevertheless, these data are consistent with Golgi accumulation of the Kir2.1 Andersen–Tawil mutant (Ma *et al.*, 2011).

Vacuole targeting of proteins via ESCRT requires ubiquitination by Rsp5 or Tul1 (Helliwell *et al.*, 2001; Hicke and Dunn, 2003; Dupre *et al.*, 2004; Katzmann *et al.*, 2004; Pizzirusso and Chang, 2004; Wang *et al.*, 2011). Rsp5 is an essential protein, so it would have been absent from our screen, but the Rsp5 adaptor proteins Bsd2 and Tre1, which regulate the trafficking and stability of plasma membrane and Golgi proteins, were identified (Portnoy *et al.*, 2000; Hettema *et al.*, 2004; Stimpson *et al.*, 2006). Consistent with these results, the plasma membrane–resident population of Kir2.1 is most likely regulated by ubiquitin conjugation (Alesutan *et al.*, 2011).

The rescue of a *trk1*Δ*trk2*Δ strain on low potassium when each of the identified genes was deleted was mediated by Kir2.1 function and is not simply a result of the deleted gene making the yeast more tolerant to potassium-poor medium. For each hit, we showed that the introduction of a vector control was unable to improve growth to the same level as a strain expressing Kir2.1. However, a screen for mutants that exhibited increased sensitivity to cationic drugs identified Arl1, the COG complex, the GARP complex, and retromer (Barreto *et al.*, 2011), suggesting that some of hits from our screen may alter the localization of other yeast potassium channels in addition to Kir2.1. Many of our hits also lead to increased CPY secretion (Bonangelino *et al.*, 2002). However, the strains that increase CPY secretion do not completely overlap with the hits identified in this study; thus Kir2.1 localization is regulated differently than this soluble, vacuolar-resident protein (see Supplemental Table S1). In fact, there is more overlap with genes identified in a screen for mutants that rescue the localization of a defective form of the plasma membrane ATPase Pma1 (e.g., Vps38, Vps36, Vps29, Vps13, Vps35, Vps27, and Bsd2; Luo and Chang, 1997). A screen was also performed in which another inward-rectifying potassium channel, Kir3.2, was mutated so that it was sodium selective, and strains expressing the protein were crossed to a subset of the deletion collection (Haass *et al.*, 2007). The resulting haploids were screened on medium containing high sodium, and seven genes associated with COPII-dependent transport and lipid biogenesis were identified that, when mutated, reduced sodium-mediated toxicity.

Our data contribute to a growing number of substrates that are regulated by the PQC machinery at the Golgi and plasma membrane in yeast (Chang and Fink, 1995; Hong *et al.*, 1996; Jenness *et al.*, 1997; Haynes *et al.*, 2002; Spear and Ng, 2003; Coughlan *et al.*, 2004; Wang and Ng, 2010) and mammals (Armstrong *et al.*, 1990; Ashok and Hegde, 2009; Apaja *et al.*, 2010; Okiyoneda *et al.*, 2010). It is worthwhile to note that the population of an unrelated potassium channel, KCa3.1, at the plasma membrane is also regulated by ESCRT and that mutant forms of this channel are subject to ERAD (Balut *et al.*, 2012). Therefore in the future it will be interesting to determine whether ESCRT is used for the targeted destruction of all or only a subset of potassium and perhaps other ion channels. In addition, we found that a core collection of Hsp70 and Hsp40 molecular chaperones aid in the identification of Kir2.1 as an ERAD substrate in the ER. Studies in mammalian cells identified Hsc70, Hsp90, and Hsp40s as important for the recognition of the CFTR mutant that resides at the plasma membrane (Okiyoneda *et al.*, 2010). Future work will uncover whether these and other chaperones operate at multiple quality control networks for Kir2.1 and other ion transporters.

MATERIALS AND METHODS

Yeast strains and growth conditions

Yeast strains were propagated at 26°C, and standard methods for growth, media preparation, and transformation were used unless indicated otherwise (Adams *et al.*, 1998). Yeast with plasmids containing constitutive promoters (*GPD* or *TEF*) were grown in selective medium and harvested at the OD_{600} indicated in each experiment. Yeast harboring plasmids containing the *MET25* promoter were maintained on medium containing 0.5 mM methionine to inhibit protein synthesis. To induce Kir2.1 expression, cells were grown to log phase in selective medium supplemented with methionine, collected by centrifugation and washed in sterile water, and then resuspended in selective medium lacking methionine for 1–2 h. After induction, cells were used as described for each experiment. For low-potassium growth assays and the SGA screen, 20 mM MES (2-(*N*-morpholino)ethanesulfonic acid) and the indicated concentration of potassium were added. Medium was also prepared at the desired pH with Tris-HCl. A complete list of the strains used in this study is presented in Supplemental Table S2.

For growth assays, 5-ml cultures were grown to log phase in synthetic complete medium lacking leucine (SC-Leu) but containing 100 mM KCl at 30°C, and 1 OD_{600} of cells was collected by centrifugation. The yeast were resuspended in 500 µl of sterile water. Cells were serially diluted 10-fold, plated using a 32-pin manifold onto SC-Leu medium containing 0, 10, 25, or 100 mM KCl, and grown at 30°C for 2 d. Plates were imaged using an Epson Perfection 3490 Photo Scanner. To assay protein expression, an equal number of cells was taken from the plates, and total protein was precipitated with 10% trichloroacetic acid and resolved by SDS–PAGE before Western blot analysis (Zhang *et al.*, 2001). Kir2.1 was detected using an anti–HA-horseradish peroxidase (HRP)–conjugated antibody, and blots were probed with anti–glucose-6-phosphate dehydrogenase (G6PD) antiserum to provide a loading control. The G6PD primary antibody was decorated with donkey HRP-conjugated anti–rabbit immunoglobulin G secondary antibody. The Supersignal Chemiluminescent Substrate (Pierce, Rockford, IL) was used to develop the blots, and the signals were quantified using a Kodak 440CF Image Station and the associated Kodak 1D software (Eastman Kodak, Rochester, NY).

Strain YAK01 (Supplemental Table S2) was constructed from Y7029 by homologous recombination (Brachmann *et al.*, 1998). The NAT cassette was PCR amplified using primers oAK01 and oAK02 (Supplemental Table S3), which also contained homology to the *TRK2* locus, and the PCR product was used to delete *TRK2* in Y7029. The *URA3* cassette from pRS426 (Mumberg *et al.*, 1995) was PCR amplified using primers oAK05 and oAK06 (Supplemental Table S3), which contained homology to the *TRK1* locus. The product was then used to delete *TRK1* in Y7029. YAK02 and YAK03 were constructed from AK01 by mating this strain with a *vps23*Δ and a *doa10*Δ mutant from the yeast deletion collection (Invitrogen, Carlsbad, CA), respectively. All constructed strains were confirmed by growth on selective medium and by PCR using specific primers (Supplemental Table S3). *CDC48* and *cdc48-2* were constructed by mating *cdc48-2* (Li *et al.*, 2011) to *ybr074*Δ (Invitrogen), and the identity of the desired genotype was confirmed by plating on medium containing G418 (Research Products International, Mount Prospect, IL) and sequencing after PCR amplification of the locus.

Plasmid construction

Mouse Kir2.1 in pcDNA3.1 was modified with an internal HA tag that was positioned so that it faced the extracellular space (Ma *et al.*, 2001). To create a yeast Kir2.1-HA expression construct with a C-terminal myc tag (myc-Kir2.1-HA), the Kir2.1 coding sequence within the pcDNA3.1 vector was PCR amplified using the PCR Master Mix reagent (Fermentas, Waltham, MA). The amplified Kir2.1 sequence was purified using the PureLink PCR purification kit (Invitrogen) and ligated into the pGEM-T easy vector (Promega, Madison, WI). The pGEM-T-Kir2.1 plasmids were sequenced to identify clones that contained the correct Kir2.1 insert. The insert was removed from pGEM-T using *Eco*RI, the fragment was gel purified using PureLink Quick Gel Extraction Kit (Invitrogen), and the isolated species was ligated into the *Eco*RI site of yeast plasmids containing either constitutive (*TEF*, *GPD*) or regulated (*MET25*) promoters (Mumberg *et al.*, 1994, 1995). The myc-Kir2.1-HA insert was then cloned into digested pRS vectors containing different promoters and genes for auxotrophic selection (Mumberg *et al.*, 1994, 1995) using *Sma*I and *Xho*I. The cut vector was treated with Antarctic phosphatase (New England BioLabs, Ipswich, MA), and the digested vectors were run on a 1% agarose gel and purified with PureLink Quick Gel Extraction Kit (Invitrogen). The cut vectors and inserts were finally ligated using T4 DNA Ligase (Fermentas). Kir2.1-AAA and Kir2.1Δ314-315 were made by two-stage PCR mutagenesis (Vallejo *et al.*, 1994). The Kir2.1 mutated cassettes were then inserted into the PRS415TEF vectors as described. All isolated inserts were subject to DNA sequence analysis.

Genetic screening conditions

The query strain (YAK01) was mated to the *MAT***a** strain deletion collection (Invitrogen) as described (Tong and Boone, 2006). In brief, the query strain was plated onto SC-Leu plates using a 96-pin manifold (Aladin Enterprises, Brisbane, CA). Strains in the deletion collection were then plated over the query strain, and the plates were incubated at 30°C for 1 d. The cells were next plated onto SC-Leu containing 200 mg/l G418 (Research Products International), 100 mg/l clonNAT (Werner BioAgents, Jena, Germany), and 100 mM KCl to select for diploids and to maintain a potassium-sensitive phenotype and were incubated at 30°C for 2 d. The resulting diploid cells were plated onto sporulation medium and kept at room temperature for 5 d. Finally, the spores were inoculated on diploid selection media lacking histidine, arginine, and uracil and containing 50 mg/l canavanine (Sigma-Aldrich, St. Louis, MO) and were incubated at 30°C for 2 d. This step was repeated two additional times with 1-d incubations to select against any remaining diploids. The final haploid strains, each expressing Kir2.1 but deleted for *TRK1*, *TRK2*, and one of 4847 genes in the collection, were screened on SC-Leu medium lacking any added potassium and were examined after 2 d at 30°C.

Colonies that grew significantly better than the average colony size on the plate were verified by growth in liquid medium at 30°C in a 96-well plate. Initial cultures were grown in 200 µl of SC-Leu medium containing 100 mM KCl. A total of 5 µl of the initial cultures was pipetted into 195 µl of SC-Leu medium lacking KCl and grown at 30°C with shaking. The OD_{600} was measured every 1–2 h with a Thermo Scientific (Waltham, MA) Multiskan Go plate reader to obtain the doubling times. All experiments were performed in triplicate.

Indirect immunofluorescence in yeast

Yeast cells expressing Kir2.1 were grown to an OD_{600} of 0.5–0.8 and fixed with 3.7% formaldehyde for 1 h at 30°C. The cells were then collected by centrifugation and washed with solution A (2 M sorbitol, 0.5 M KPO_4, pH 7) and resuspended in 500 µl of solution A supplemented with 60 ng/ml 100T Zymolyase (MP Biomedicals, Solon, OH) and 25 mM 2-mercaptoethanol and were incubated at 37°C for 30 min. The spheroplasts were pelleted at 3000 rpm for 3 min, washed with solution A, and resuspended in 800 µl of solution A. The cell suspension (30 µl) was added to a microscope slide well (pretreated with 1 mg/ml polylysine) and incubated at room temperature for 30 min. The liquid was aspirated, and the wells were washed once with phosphate-buffered saline (PBS)/0.1% bovine serum albumin (BSA) and twice with PBS/0.1% BSA/0.1% NP40 and then incubated with the following primary antibodies at 4°C: anti-HA at a 1:250 dilution and anti-Kar2 at a 1:500 dilution. The slides were next washed once with PBS/0.1% BSA, once with PBS/0.1%BSA/0.1% NP40, and once with PBS/0.1% BSA and were incubated with the appropriate secondary antibodies (Alexa Fluor 568 goat anti-rabbit and Alexa Fluor 488 goat anti-mouse; Molecular Probes, Eugene, OR) in PBS/0.1% BSA for 1 h at room temperature. The slides were again washed as described, and coverslips were mounted using ProLong Gold Antifade mounting media (Invitrogen). Images were captured on an Olympus BX60 microscope (Olympus, Tokyo, Japan) fitted with a Hamamatsu C4742–95 digital camera (Hamamatsu, Bridgewater, NJ), using QED Imaging software (Media Cybernetics, Silver Spring, MD).

Biochemical assays

Kir2.1 degradation was assayed by cycloheximide chase analysis as described (Buck *et al.*, 2010). In brief, cells expressing Kir2.1 under the control of the *GPD* promoter were grown in selective medium with shaking to log phase (OD_{600} 0.4–1.2), and 100 µg/ml of cycloheximide (Sigma-Aldrich) was added to stop protein translation. The yeast were incubated at 30°C in a shaking water bath, and temperature-sensitive mutants were incubated at 37°C for 10 min before performing the chase at 37°C. The *cdc48-2* temperature-sensitive strain and the isogenic wild type were incubated at 39°C for 2 h before the start of the chase, and the incubation was continued at 39°C. A 1-ml aliquot of the culture was collected at the indicated time points, and pelleted cells were washed with ice-cold water containing protease inhibitors, flash-frozen in liquid nitrogen, and stored at –80°C. Total protein was precipitated from samples as described (Zhang *et al.*, 2001) and immediately resolved by SDS–PAGE before Western blot analysis, as described.

To measure the relative amount of Kir2.1 ubiquitination, cells harboring the pRS426MET25-Kir2.1 plasmid were grown to an OD_{600} of 1.0 in 50-ml cultures of selective medium containing 0.5 mM methionine. The yeast were collected by centrifugation, washed in sterile water, and resuspended in the same medium lacking methionine for 2 h. After induction, the cells were collected by centrifugation and quick frozen in liquid nitrogen and stored at –80°C until use. Immunoprecipitations were preformed essentially as described (Ahner *et al.*, 2007). In brief, cells were broken by glass-bead lysis, and membranes were collected by centrifugation. The membranes were then treated with SDS buffer to liberate Kir2.1, and after dilution into a Triton X-100–containing buffer an anti-HA antibody conjugated to agarose beads (Pierce) was added and the slurry was incubated overnight with rocking at 4°C. The beads were washed, and SDS sample buffer was used to liberate the bound proteins. The released proteins were subjected to SDS–PAGE and Western blot analysis to detect total Kir2.1 and the ubiquitinated Kir2.1 fraction.

The intracellular residence of Kir2.1 was determined by sedimentation in a sucrose gradient essentially as described (Sullivan

et al., 2003). A 40-ml culture was grown to an OD_{600} of 0.8, and the cells were harvested by centrifugation, resuspended in 10 mM Tris-HCl, pH 7.5, 1 mM EDTA, and 10% sucrose, and then disrupted by agitation with glass beads. The cell lysates were cleared of debris by low-speed centrifugation and the resulting lysate (300 µl) was layered at the top of a 11 ml 30–70% sucrose gradient and centrifuged at 100,000 × *g* in a Beckman SW41 rotor for 14 h at 4°C. Fractions were collected by pippeting from the top of the tube. The presence of specific proteins was analyzed by SDS–PAGE and Western blot.

Analysis of Kir2.1 in HeLa Cells

HeLa cells were cultured in DMEM with 10% FBS, 100 U/ml penicillin/streptomycin, and 2 mM glutamine at 37°C and 5% CO_2. XtremeGENE9 transfection reagent (Roche, Indianapolis, IN) was used as per the manufacturer's guidelines to transfect mouse Kir2.1 in pcDNA3.1 (pcDNA3.1-HA-Kir2.1). To knock down the expression of ESCRT proteins, HeLa cells plated in six-well dishes were cotransfected with 1 µg of pcDNA3.1-HA-Kir2.1 and 2 µg of siRNA using XtremeGENE siRNA transfection reagent (Roche, Penzberg, Germany). The siRNAs for human TSG101 (CCAAAUACUUCCUACAUGC), human HRS (HGS; GAACCCACACGUCGCCUUG), and a scramble control (ON-TARGETplus nontargeting siRNA #1) were obtained from Invitrogen. After 54 h a final concentration of 100 µM leupeptin was added where indicated. After another 18 h the cells were washed with PBS and collected in 1% Triton in PBS with Protease Inhibitor Cocktail (P8340; Sigma-Aldrich). Lysates were rotated for 1 h at 4°C, followed by centrifugation at 13,000 rpm in a microcentrifuge for 5 min at 4°C. Supernatants were incubated with loading buffer for 30 min at room temperature, and proteins were analyzed by SDS–PAGE and Western blot.

To determine the extent to which Kir2.1 accumulates in MVBs in HeLa cells, Kir2.1-HA was colocalized with the MVB marker, CD63 (Escola *et al.*, 1998), using a rabbit monoclonal HA antibody and a mouse monoclonal CD63 antibody. For these studies, cells were grown on glass coverslips and then fixed (4% paraformaldehyde, 30 min, 5°C), permeabilized with 0.1% Triton X-100 (10 min, 5°C), and blocked in 5% FBS (30 min, 5°C). The cells were then incubated with the primary antibodies (1:100, 2 h, 5°C), washed, and incubated with anti-mouse and anti-rabbit Alexa Fluor–conjugated secondary antibodies (1:250) for 1 h at room temperature. After washing, the cells were mounted in VectaShield (Vector Laboratories, Burlingame, CA) mounting media containing the nuclear marker 4′,6-diamidino-2-phenylindole (DAPI). The signals corresponding to each protein were visualized with a Zeiss 510 confocal microscope using a 63× oil immersion lens (numerical aperture 1.4), and images were processed using Volocity image analysis software (PerkinElmer, Boston, MA).

For immunoblot analysis, the cells were washed with PBS and collected in 1% Triton X-100 in PBS with Protease Inhibitor Cocktail and then incubated with rotation for 1 h at 4°C and centrifuged (13,000 rpm, 5 min, 4°C in a microcentrifuge) to pellet-insoluble material. Supernatant protein concentration was determined by BCA Protein Assay Kit (Pierce), and proteins were resolved by SDS–PAGE, transferred to a nitrocellulose membrane, and probed with the appropriate primary and HRP-conjugated secondary antibodies. SuperSignal West Pico Chemiluminescent Substrate was used to detect the signal from the HRP-conjugated antibody, and the chemiluminescent signal was visualized by fluorography. Densitometric measurements were made in the linear range using ImageJ (National Institutes of Health, Bethesda, MD).

To monitor Kir2.1 stability by cycloheximide chase analysis, a final concentration of 50 µg/ml cycloheximide (Sigma-Aldrich) in the presence or absence of 15 µg/ml MG132 (Peptides International, Louisville, KY) was added to cells expressing Kir2.1-HA to stop protein translation and inhibit the proteasome, respectively. The cells were incubated at 37°C and harvested with 100 µl of lysis buffer (50 mM Tris, pH 7.2, 1% Triton X-100, 150 mM NaCl, cOmplete Mini protease inhibitor cocktail [Roche Diagnostics]), and the protein concentration was measured by bicinchoninic acid (Thermo Scientific). Equal amounts of protein were resolved by SDS–PAGE before Western blot analysis.

To assess the turnover of Kir2.1 using a metabolic pulse-chase protocol, HeLa cells were transfected with pcDNA3.1 HA-Kir2.1 and treated with 100 µM leupeptin immediately after transfection and again 6 h later. The following day, fresh leupeptin was added to DMEM lacking cysteine and methionine (Sigma-Aldrich), and cells were starved for 45 min, followed by a 1-h pulse with 125 µCi/ml EasyTag Express ^{35}S protein labeling mix (PerkinElmer). After the pulse, the cells were chilled to 4°C using an ice-cold metal plate and washed three times for 5 min each with DMEM containing 5 mM cysteine and methionine and 10 mM 4-(2-hydroxyethyl)-1-piperazineethanesulfonic acid, pH 7.4. The cells were then incubated with prewarmed chase media supplemented with 0.2% dimethylsulfoxide or 100 µM leupeptin. Leupeptin was readded at 3 and 6 h of the chase. At each measured time point, the cells were cooled by washing with ice-cold PBS, followed by solubilization with 500 µl of detergent solution (50 mM Tris, pH 8, 100 mM EDTA, pH 8, 0.4% sodium deoxycholate, 1% Nonidet P-40, protease inhibitors [1 mM phenylmethylsulfonyl fluoride, 1 µg/ml leupeptin, and 0.5 µg/ml pepstatin A]). The resulting lysates were centrifuged for 10 min at 17,000 × *g* in a refrigerated microcentrifuge, and the postnuclear supernatants were transferred to a fresh tube containing 10 µg of mouse anti-HA (12CA5; Roche) and rotated overnight at 4°C. Antibody-Kir2.1 complexes were captured using fixed *Staphylococcus aureus* (Pansorbin; Calbiochem, San Diego, CA) and washed three times with 10 mM Tris-HCl, 0.15 M NaCl, 1% Triton X-100, 1% Nonidet P-40, and 0.1% SDS, pH 7.4. Samples were eluted with SDS sample buffer supplemented with 5% β-mercaptoethanol and electrophoresed using 10% SDS–PAGE. The gels were dried and exposed to a phosphorimager screen before analysis using Image J.

Statistical analysis

To analyze experiments performed in HeLa cells (Figure 6), statistical analysis was performed using Prism (GraphPad, La Jolla, CA). Statistical significance was determined by one-way analysis of variance (ANOVA) and Tukey's post hoc test in G and two-way ANOVA and Bonferroni post tests in H.

Antibodies

The following primary antibodies were used for studies in yeast: HRP-conjugated rat monoclonal anti-HA high-affinity (3F10; Roche), anti-HA mouse monoclonal (Roche), G6PD rabbit polyclonal antibody (Sigma-Aldrich), a ubiquitin (P4D1) mouse monoclonal antibody from Santa Cruz (Dallas, TX; sc-8017), and a polyclonal rabbit anti-Kar2 (Brodsky and Schekman, 1993). A polyclonal rabbit anti-Pma1 was a gift from Amy Chang (University of Michigan, Ann Arbor, MI). The following secondary antibodies were used in yeast: HRP-conjugated goat anti-mouse and goat anti-rabbit antibodies (Jackson ImmunoResearch, West Grove, PA) and Alexa Fluor 568 goat anti-rabbit and Alexa Fluor 488 goat anti-mouse (Invitrogen,

Carlsbad, CA). The following antibodies were used for studies in HeLa cells: HA mouse monoclonal antibody (Covance, Princeton, NJ), HA rabbit monoclonal antibody (Cell Signaling, Danvers, MA), CD63 mouse monoclonal antibody (Invitrogen), TSG101 mouse monoclonal antibody (GeneTex, Irvine, CA), HRS (HGS) mouse monoclonal antibody (Abcam), and VPS35 goat polyclonal antibody (Abcam). The following secondary antibodies were used for immunofluorescence studies in HeLa cells: anti-mouse and anti-rabbit Alexa Fluor–conjugated secondary antibodies (Molecular Probes).

ACKNOWLEDGMENTS

We thank the laboratories of Rick Gaber, Lily Jan, Amy Chang, Elizabeth Miller, Ed Levitan, and Joseph Martens for reagents and technical advice. We also thank Linton Traub, Tom Kleyman, Ora Weisz, and Karen Arndt for helpful suggestions during the course of these studies. A.R.K. acknowledges support from American Heart Association Pre-doctoral Fellowship 09PRE2050048. This work was supported by Grants GM75061, DK65161, and DK79307 (University of Pittsburgh George O'Brien Kidney Research Core Center) from the National Institutes of Health to J.L.B. and National Institutes of Health Grants DK63049 and DK54231 to P.A.W.

REFERENCES

Adams A, Gottschling DE, Kaiser CA, Stearns T (1998). Methods in Yeast Genetics: A Cold Spring Harbor Laboratory Course Manual, Plainview, NY: Cold Spring Harbor Laboratory Press.

Aebi M, Bernasconi R, Clerc S, Molinari M (2010). N-glycan structures: recognition and processing in the ER. Trends Biochem Sci 35, 74–82.

Ahner A, Nakatsukasa K, Zhang H, Frizzell RA, Brodsky JL (2007). Small heat-shock proteins select deltaF508-CFTR for endoplasmic reticulum-associated degradation. Mol Biol Cell 18, 806–814.

Alesutan I, Munoz C, Sopjani M, Dermaku-Sopjani M, Michael D, Fraser S, Kemp BE, Seebohm G, Foller M, Lang F (2011). Inhibition of Kir2.1 (KCNJ2) by the AMP-activated protein kinase. Biochem Biophys Res Commun 408, 505–510.

Apaja PM, Xu H, Lukacs GL (2010). Quality control for unfolded proteins at the plasma membrane. J Cell Biol 191, 553–570.

Armstrong J, Patel S, Riddle P (1990). Lysosomal sorting mutants of coronavirus E1 protein, a Golgi membrane protein. J Cell Sci 95 (Pt 2), 191–197.

Arvan P, Zhao X, Ramos-Castaneda J, Chang A (2002). Secretory pathway quality control operating in Golgi, plasmalemmal, and endosomal systems. Traffic 3, 771–780.

Ashok A, Hegde RS (2009). Selective processing and metabolism of disease-causing mutant prion proteins. PLoS Pathog 5, e1000479.

Azmi IF, Davies BA, Xiao J, Babst M, Xu Z, Katzmann DJ (2008). ESCRT-III family members stimulate Vps4 ATPase activity directly or via Vta1. Dev Cell 14, 50–61.

Babst M, Odorizzi G, Estepa EJ, Emr SD (2000). Mammalian tumor susceptibility gene 101 (TSG101) and the yeast homologue, Vps23p, both function in late endosomal trafficking. Traffic 1, 248–258.

Babst M, Wendland B, Estepa EJ, Emr SD (1998). The Vps4p AAA ATPase regulates membrane association of a Vps protein complex required for normal endosome function. EMBO J 17, 2982–2993.

Balut CM, Hamilton KL, Devor DC (2012). Trafficking of intermediate (KCa3.1) and small (KCa2.x) conductance, Ca(2+)-activated K(+) channels: a novel target for medicinal chemistry efforts. Chem Med Chem 7, 1741–1755.

Barreto L *et al*. (2011). A genomewide screen for tolerance to cationic drugs reveals genes important for potassium homeostasis in *Saccharomyces cerevisiae*. Eukaryot Cell 10, 1241–1250.

Behnia R, Panic B, Whyte JR, Munro S (2004). Targeting of the Arf-like GTPase Arl3p to the Golgi requires N-terminal acetylation and the membrane protein Sys1p. Nat Cell Biol 6, 405–413.

Bilodeau PS, Urbanowski JL, Winistorfer SC, Piper RC (2002). The Vps27p Hse1p complex binds ubiquitin and mediates endosomal protein sorting. Nat Cell Biol 4, 534–539.

Bonangelino CJ, Chavez EM, Bonifacino JS (2002). Genomic screen for vacuolar protein sorting genes in *Saccharomyces cerevisiae*. Mol Biol Cell 13, 2486–2501.

Brachmann CB, Davies A, Cost GJ, Caputo E, Li J, Hieter P, Boeke JD (1998). Designer deletion strains derived from *Saccharomyces cerevisiae* S288C: a useful set of strains and plasmids for PCR-mediated gene disruption and other applications. Yeast 14, 115–132.

Brodsky JL, Schekman R (1993). A Sec63p-BiP complex from yeast is required for protein translocation in a reconstituted proteoliposome. J Cell Biol 123, 1355–1363.

Brodsky JL, Werner ED, Dubas ME, Goeckeler JL, Kruse KB, McCracken AA (1999). The requirement for molecular chaperones during endoplasmic reticulum-associated protein degradation demonstrates that protein export and import are mechanistically distinct. J Biol Chem 274, 3453–3460.

Buck TM, Kolb AR, Boyd CR, Kleyman TR, Brodsky JL (2010). The endoplasmic reticulum-associated degradation of the epithelial sodium channel requires a unique complement of molecular chaperones. Mol Biol Cell 21, 1047–1058.

Burda P, Padilla SM, Sarkar S, Emr SD (2002). Retromer function in endosome-to-Golgi retrograde transport is regulated by the yeast Vps34 PtdIns 3-kinase. J Cell Sci 115, 3889–3900.

Carvalho P, Goder V, Rapoport TA (2006). Distinct ubiquitin-ligase complexes define convergent pathways for the degradation of ER proteins. Cell 126, 361–373.

Chang A, Fink GR (1995). Targeting of the yeast plasma membrane [H+] ATPase: a novel gene AST1 prevents mislocalization of mutant ATPase to the vacuole. J Cell Biol 128, 39–49.

Claessen JH, Kundrat L, Ploegh HL (2012). Protein quality control in the ER: balancing the ubiquitin checkbook. Trends Cell Biol 22, 22–32.

Conibear E, Stevens TH (2000). Vps52p, Vps53p, and Vps54p form a novel multisubunit complex required for protein sorting at the yeast late Golgi. Mol Biol Cell 11, 305–323.

Coughlan CM, Walker JL, Cochran JC, Wittrup KD, Brodsky JL (2004). Degradation of mutated bovine pancreatic trypsin inhibitor in the yeast vacuole suggests post-endoplasmic reticulum protein quality control. J Biol Chem 279, 15289–15297.

Dang H, Klokk TI, Schaheen B, McLaughlin BM, Thomas AJ, Durns TA, Bitler BG, Sandvig K, Fares H (2011). Derlin-dependent retrograde transport from endosomes to the Golgi apparatus. Traffic 12, 1417–1431.

de Boer TP, Houtman MJ, Compier M, van der Heyden MA (2010). The mammalian K(IR)2.x inward rectifier ion channel family: expression pattern and pathophysiology. Acta Physiol (Oxf) 199, 243–256.

Denic V, Quan EM, Weissman JS (2006). A luminal surveillance complex that selects misfolded glycoproteins for ER-associated degradation. Cell 126, 349–359.

Dupre S, Urban-Grimal D, Haguenauer-Tsapis R (2004). Ubiquitin and endocytic internalization in yeast and animal cells. Biochim Biophys Acta 1695, 89–111.

Escola JM, Kleijmeer MJ, Stoorvogel W, Griffith JM, Yoshie O, Geuze HJ (1998). Selective enrichment of tetraspan proteins on the internal vesicles of multivesicular endosomes and on exosomes secreted by human B-lymphocytes. J Biol Chem 273, 20121–20127.

Fisher EA, Khanna NA, McLeod RS (2011). Ubiquitination regulates the assembly of VLDL in HepG2 cells and is the committing step of the apoB-100 ERAD pathway. J Lipid Res 52, 1170–1180.

Gestwicki JE, Garza D (2012). Protein quality control in neurodegenerative disease. Prog Mol Biol Transl Sci 107, 327–353.

Gill DJ, Teo H, Sun J, Perisic O, Veprintsev DB, Emr SD, Williams RL (2007). Structural insight into the ESCRT-I/-II link and its role in MVB trafficking. EMBO J 26, 600–612.

Grove DE, Rosser MF, Ren HY, Naren AP, Cyr DM (2009). Mechanisms for rescue of correctable folding defects in CFTRDelta F508. Mol Biol Cell 20, 4059–4069.

Guerriero CJ, Brodsky JL (2012). The delicate balance between secreted protein folding and endoplasmic reticulum-associated degradation in human physiology. Physiol Rev 92, 537–576.

Haass FA, Jonikas M, Walter P, Weissman JS, Jan YN, Jan LY, Schuldiner M (2007). Identification of yeast proteins necessary for cell-surface function of a potassium channel. Proc Natl Acad Sci USA 104, 18079–18084.

Halaban R, Cheng E, Zhang Y, Moellmann G, Hanlon D, Michalak M, Setaluri V, Hebert DN (1997). Aberrant retention of tyrosinase in the endoplasmic reticulum mediates accelerated degradation of the enzyme and contributes to the dedifferentiated phenotype of amelanotic melanoma cells. Proc Natl Acad Sci USA 94, 6210–6215.

Han S, Liu Y, Chang A (2007). Cytoplasmic Hsp70 promotes ubiquitination for endoplasmic reticulum-associated degradation of a misfolded

mutant of the yeast plasma membrane ATPase, PMA1. J Biol Chem 282, 26140–26149.
Haynes CM, Caldwell S, Cooper AA (2002). An HRD/DER-independent ER quality control mechanism involves Rsp5p-dependent ubiquitination and ER-Golgi transport. J Cell Biol 158, 91–101.
Hebert DN, Molinari M (2012). Flagging and docking: dual roles for N-glycans in protein quality control and cellular proteostasis. Trends Biochem Sci 37, 404–410.
Helliwell SB, Losko S, Kaiser CA (2001). Components of a ubiquitin ligase complex specify polyubiquitination and intracellular trafficking of the general amino acid permease. J Cell Biol 153, 649–662.
Hettema EH, Valdez-Taubas J, Pelham HR (2004). Bsd2 binds the ubiquitin ligase Rsp5 and mediates the ubiquitination of transmembrane proteins. EMBO J 23, 1279–1288.
Hibino H, Inanobe A, Furutani K, Murakami S, Findlay I, Kurachi Y (2010). Inwardly rectifying potassium channels: their structure, function, and physiological roles. Physiol Rev 90, 291–366.
Hicke L, Dunn R (2003). Regulation of membrane protein transport by ubiquitin and ubiquitin-binding proteins. Annu Rev Cell Dev Biol 19, 141–172.
Hill K, Cooper AA (2000). Degradation of unassembled Vph1p reveals novel aspects of the yeast ER quality control system. EMBO J 19, 550–561.
Hong E, Davidson AR, Kaiser CA (1996). A pathway for targeting soluble misfolded proteins to the yeast vacuole. J Cell Biol 135, 623–633.
Huang CL, Feng S, Hilgemann DW (1998). Direct activation of inward rectifier potassium channels by PIP2 and its stabilization by Gbetagamma. Nature 391, 803–806.
Huotari J, Helenius A (2011). Endosome maturation. EMBO J 30, 3481–3500.
Hurtley SM, Helenius A (1989). Protein oligomerization in the endoplasmic reticulum. Annu Rev Cell Biol 5, 277–307.
Jansen JA, de Boer TP, Wolswinkel R, van Veen TA, Vos MA, van Rijen HV, van der Heyden MA (2008). Lysosome mediated Kir2.1 breakdown directly influences inward rectifier current density. Biochem Biophys Res Commun 367, 687–692.
Jenness DD, Li Y, Tipper C, Spatrick P (1997). Elimination of defective alpha-factor pheromone receptors. Mol Cell Biol 17, 6236–6245.
Katzmann DJ, Sarkar S, Chu T, Audhya A, Emr SD (2004). Multivesicular body sorting: ubiquitin ligase Rsp5 is required for the modification and sorting of carboxypeptidase S. Mol Biol Cell 15, 468–480.
Keener JM, Babst M (2013). Quality control and substrate-dependent downregulation of the nutrient transporter Fur4. Traffic 14, 412–427.
Kihara A, Noda T, Ishihara N, Ohsumi Y (2001). Two distinct Vps34 phosphatidylinositol 3-kinase complexes function in autophagy and carboxypeptidase Y sorting in *Saccharomyces cerevisiae*. J Cell Biol 152, 519–530.
Kim Y, Deng Y, Philpott CC (2007). GGA2- and ubiquitin-dependent trafficking of Arn1, the ferrichrome transporter of *Saccharomyces cerevisiae*. Mol Biol Cell 18, 1790–1802.
Kincaid MM, Cooper AA (2007). Misfolded proteins traffic from the endoplasmic reticulum (ER) due to ER export signals. Mol Biol Cell 18, 455–463.
Komada M, Masaki R, Yamamoto A, Kitamura N (1997). Hrs, a tyrosine kinase substrate with a conserved double zinc finger domain, is localized to the cytoplasmic surface of early endosomes. J Biol Chem 272, 20538–20544.
Korolchuk VI, Schutz MM, Gomez-Llorente C, Rocha J, Lansu NR, Collins SM, Wairkar YP, Robinson IM, O'Kane CJ (2007). *Drosophila* Vps35 function is necessary for normal endocytic trafficking and actin cytoskeleton organisation. J Cell Sci 120, 4367–4376.
Kostelansky MS, Schluter C, Tam YY, Lee S, Ghirlando R, Beach B, Conibear E, Hurley JH (2007). Molecular architecture and functional model of the complete yeast ESCRT-I heterotetramer. Cell 129, 485–498.
Li B, Warner JR (1996). Mutation of the Rab6 homologue of *Saccharomyces cerevisiae*, YPT6, inhibits both early Golgi function and ribosome biosynthesis. J Biol Chem 271, 16813–16819.
Li Y, Kane T, Tipper C, Spatrick P, Jenness DD (1999). Yeast mutants affecting possible quality control of plasma membrane proteins. Mol Cell Biol 19, 3588–3599.
Li Z *et al.* (2011). Systematic exploration of essential yeast gene function with temperature-sensitive mutants. Nat Biotechnol 29, 361–367.
Lu C, Jiang C, Pribanic S, Rotin D (2007). CFTR stabilizes ENaC at the plasma membrane. J Cyst Fibros 6, 419–422.
Luo W, Chang A (1997). Novel genes involved in endosomal traffic in yeast revealed by suppression of a targeting-defective plasma membrane ATPase mutant. J Cell Biol 138, 731–746.
Ma D, Taneja TK, Hagen BM, Kim BY, Ortega B, Lederer WJ, Welling PA (2011). Golgi export of the Kir2.1 channel is driven by a trafficking signal located within its tertiary structure. Cell 145, 1102–1115.
Ma D, Zerangue N, Lin YF, Collins A, Yu M, Jan YN, Jan LY (2001). Role of ER export signals in controlling surface potassium channel numbers. Science 291, 316–319.
Makuc J, Cappellaro C, Boles E (2004). Co-expression of a mammalian accessory trafficking protein enables functional expression of the rat MCT1 monocarboxylate transporter in *Saccharomyces cerevisiae*. FEMS Yeast Res 4, 795–801.
Mayers JR, Fyfe I, Schuh AL, Chapman ER, Edwardson JM, Audhya A (2011). ESCRT-0 assembles as a heterotetrameric complex on membranes and binds multiple ubiquitinylated cargoes simultaneously. J Biol Chem 286, 9636–9645.
McCullough J, Row PE, Lorenzo O, Doherty M, Beynon R, Clague MJ, Urbe S (2006). Activation of the endosome-associated ubiquitin isopeptidase AMSH by STAM, a component of the multivesicular body-sorting machinery. Curr Biol 16, 160–165.
Mehnert M, Sommer T, Jarosch E (2010). ERAD ubiquitin ligases: multifunctional tools for protein quality control and waste disposal in the endoplasmic reticulum. Bioessays 32, 905–913.
Minor DL Jr, Masseling SJ, Jan YN, Jan LY (1999). Transmembrane structure of an inwardly rectifying potassium channel. Cell 96, 879–891.
Mitchell DM, Zhou M, Pariyarath R, Wang H, Aitchison JD, Ginsberg HN, Fisher EA (1998). Apoprotein B100 has a prolonged interaction with the translocon during which its lipidation and translocation change from dependence on the microsomal triglyceride transfer protein to independence. Proc Natl Acad Sci USA 95, 14733–14738.
Montpetit B, Conibear E (2009). Identification of the novel TRAPP associated protein Tca17. Traffic 10, 713–723.
Mumberg D, Muller R, Funk M (1994). Regulatable promoters of *Saccharomyces cerevisiae*: comparison of transcriptional activity and their use for heterologous expression. Nucleic Acids Res 22, 5767–5768.
Mumberg D, Muller R, Funk M (1995). Yeast vectors for the controlled expression of heterologous proteins in different genetic backgrounds. Gene 156, 119–122.
Nakamura RL, Gaber RF (1998). Studying ion channels using yeast genetics. Methods Enzymol 293, 89–104.
Nakatsukasa K, Huyer G, Michaelis S, Brodsky JL (2008). Dissecting the ER-associated degradation of a misfolded polytopic membrane protein. Cell 132, 101–112.
Nalos L, de Boer TP, Houtman MJ, Rook MB, Vos MA, van der Heyden MA (2011). Inhibition of lysosomal degradation rescues pentamidine-mediated decreases of K(IR)2.1 ion channel expression but not that of K(v)11.1. Eur J Pharmacol 652, 96–103.
Obara K, Sekito T, Ohsumi Y (2006). Assortment of phosphatidylinositol 3-kinase complexes–Atg14p directs association of complex I to the pre-autophagosomal structure in *Saccharomyces cerevisiae*. Mol Biol Cell 17, 1527–1539.
Okiyoneda T, Barriere H, Bagdany M, Rabeh WM, Du K, Hohfeld J, Young JC, Lukacs GL (2010). Peripheral protein quality control removes unfolded CFTR from the plasma membrane. Science 329, 805–810.
Pizzirusso M, Chang A (2004). Ubiquitin-mediated targeting of a mutant plasma membrane ATPase, Pma1–7, to the endosomal/vacuolar system in yeast. Mol Biol Cell 15, 2401–2409.
Plaster NM *et al.* (2001). Mutations in Kir2.1 cause the developmental and episodic electrical phenotypes of Andersen's syndrome. Cell 105, 511–519.
Plemper RK, Bohmler S, Bordallo J, Sommer T, Wolf DH (1997). Mutant analysis links the translocon and BiP to retrograde protein transport for ER degradation. Nature 388, 891–895.
Portnoy ME, Liu XF, Culotta VC (2000). *Saccharomyces cerevisiae* expresses three functionally distinct homologues of the nramp family of metal transporters. Mol Cell Biol 20, 7893–7902.
Priori SG *et al.* (2005). A novel form of short QT syndrome (SQT3) is caused by a mutation in the KCNJ2 gene. Circ Res 96, 800–807.
Qu D, Teckman JH, Omura S, Perlmutter DH (1996). Degradation of a mutant secretory protein, alpha1-antitrypsin Z, in the endoplasmic reticulum requires proteasome activity. J Biol Chem 271, 22791–22795.
Ram RJ, Li B, Kaiser CA (2002). Identification of Sec36p, Sec37p, and Sec38p: components of yeast complex that contains Sec34p and Sec35p. Mol Biol Cell 13, 1484–1500.
Reggiori F, Pelham HR (2002). A transmembrane ubiquitin ligase required to sort membrane proteins into multivesicular bodies. Nat Cell Biol 4, 117–123.

Roberg KJ, Rowley N, Kaiser CA (1997). Physiological regulation of membrane protein sorting late in the secretory pathway of *Saccharomyces cerevisiae*. J Cell Biol 137, 1469–1482.
Robinson JS, Klionsky DJ, Banta LM, Emr SD (1988). Protein sorting in *Saccharomyces cerevisiae*: isolation of mutants defective in the delivery and processing of multiple vacuolar hydrolases. Mol Cell Biol 8, 4936–4948.
Romanenko VG, Fang Y, Byfield F, Travis AJ, Vandenberg CA, Rothblat GH, Levitan I (2004). Cholesterol sensitivity and lipid raft targeting of Kir2.1 channels. Biophys J 87, 3850–3861.
Rothman JH, Stevens TH (1986). Protein sorting in yeast: mutants defective in vacuole biogenesis mislocalize vacuolar proteins into the late secretory pathway. Cell 47, 1041–1051.
Sacher M, Barrowman J, Schieltz D, Yates JR3rd, Ferro-Novick S (2000). Identification and characterization of five new subunits of TRAPP. Eur J Cell Biol 79, 71–80.
Sato BK, Schulz D, Do PH, Hampton RY (2009). Misfolded membrane proteins are specifically recognized by the transmembrane domain of the Hrd1p ubiquitin ligase. Mol Cell 34, 212–222.
Schubert U, Anton LC, Bacik I, Cox JH, Bour S, Bennink JR, Orlowski M, Strebel K, Yewdell JW (1998). CD4 glycoprotein degradation induced by human immunodeficiency virus type 1 Vpu protein requires the function of proteasomes and the ubiquitin-conjugating pathway. J Virol 72, 2280–2288.
Schwalbe RA, Rudin A, Xia SL, Wingo CS (2002). Site-directed glycosylation tagging of functional Kir2.1 reveals that the putative pore-forming segment is extracellular. J Biol Chem 277, 24382–24389.
Seaman MN, McCaffery JM, Emr SD (1998). A membrane coat complex essential for endosome-to-Golgi retrograde transport in yeast. J Cell Biol 142, 665–681.
Siniossoglou S, Pelham HR (2002). Vps51p links the VFT complex to the SNARE Tlg1p. J Biol Chem 277, 48318–48324.
Smith MH, Ploegh HL, Weissman JS (2011). Road to ruin: targeting proteins for degradation in the endoplasmic reticulum. Science 334, 1086–1090.
Spear ED, Ng DT (2003). Stress tolerance of misfolded carboxypeptidase Y requires maintenance of protein trafficking and degradative pathways. Mol Biol Cell 14, 2756–2767.
Stimpson HE, Lewis MJ, Pelham HR (2006). Transferrin receptor-like proteins control the degradation of a yeast metal transporter. EMBO J 25, 662–672.
Sullivan ML, Youker RT, Watkins SC, Brodsky JL (2003). Localization of the BiP molecular chaperone with respect to endoplasmic reticulum foci containing the cystic fibrosis transmembrane conductance regulator in yeast. J Histochem Cytochem 51, 545–548.
Tang W, Ruknudin A, Yang WP, Shaw SY, Knickerbocker A, Kurtz S (1995). Functional expression of a vertebrate inwardly rectifying K+ channel in yeast. Mol Biol Cell 6, 1231–1240.
Taxis C, Vogel F, Wolf DH (2002). ER-Golgi traffic is a prerequisite for efficient ER degradation. Mol Biol Cell 13, 1806–1818.
Teo H, Gill DJ, Sun J, Perisic O, Veprintsev DB, Vallis Y, Emr SD, Williams RL (2006). ESCRT-I core and ESCRT-II GLUE domain structures reveal role for GLUE in linking to ESCRT-I and membranes. Cell 125, 99–111.
Teo H, Perisic O, Gonzalez B, Williams RL (2004). ESCRT-II, an endosome-associated complex required for protein sorting: crystal structure and interactions with ESCRT-III and membranes. Dev Cell 7, 559–569.
Tinker A, Jan YN, Jan LY (1996). Regions responsible for the assembly of inwardly rectifying potassium channels. Cell 87, 857–868.
Tong AH, Boone C (2006). Synthetic genetic array analysis in *Saccharomyces cerevisiae*. Methods Mol Biol 313, 171–192.
Trzcinska-Daneluti AM, Ly D, Huynh L, Jiang C, Fladd C, Rotin D (2009). High-content functional screen to identify proteins that correct F508del-CFTR function. Mol Cell Proteomics 8, 780–790.
Ungar D, Oka T, Brittle EE, Vasile E, Lupashin VV, Chatterton JE, Heuser JE, Krieger M, Waters MG (2002). Characterization of a mammalian Golgi-localized protein complex, COG, that is required for normal Golgi morphology and function. J Cell Biol 157, 405–415.
Vallejo AN, Pogulis RJ, Pease LR (1994). In vitro synthesis of novel genes: mutagenesis and recombination by PCR. PCR Methods Appl 4, S123–130.
Vashist S, Kim W, Belden WJ, Spear ED, Barlowe C, Ng DT (2001). Distinct retrieval and retention mechanisms are required for the quality control of endoplasmic reticulum protein folding. J Cell Biol 155, 355–368.
Vashist S, Ng DT (2004). Misfolded proteins are sorted by a sequential checkpoint mechanism of ER quality control. J Cell Biol 165, 41–52.
Vij N, Fang S, Zeitlin PL (2006). Selective inhibition of endoplasmic reticulum-associated degradation rescues DeltaF508-cystic fibrosis transmembrane regulator and suppresses interleukin-8 levels: therapeutic implications. J Biol Chem 281, 17369–17378.
Wang S, Ng DT (2010). Evasion of endoplasmic reticulum surveillance makes Wsc1p an obligate substrate of Golgi quality control. Mol Biol Cell 21, 1153–1165.
Wang S, Thibault G, Ng DT (2011). Routing misfolded proteins through the multivesicular body (MVB) pathway protects against proteotoxicity. J Biol Chem 286, 29376–29387.
Wolf DH, Stolz A (2012). The Cdc48 machine in endoplasmic reticulum associated protein degradation. Biochim Biophys Acta 1823, 117–124.
Wollert T, Hurley JH (2010). Molecular mechanism of multivesicular body biogenesis by ESCRT complexes. Nature 464, 864–869.
Wollert T, Wunder C, Lippincott-Schwartz J, Hurley JH (2009). Membrane scission by the ESCRT-III complex. Nature 458, 172–177.
Xia WF, Tang FL, Xiong L, Xiong S, Jung JU, Lee DH, Li XS, Feng X, Mei L, Xiong WC (2013). Vps35 loss promotes hyperresorptive osteoclastogenesis and osteoporosis via sustained RANKL signaling. J Cell Biol 200, 821–837.
Zhang Y, Nijbroek G, Sullivan ML, McCracken AA, Watkins SC, Michaelis S, Brodsky JL (2001). Hsp70 molecular chaperone facilitates endoplasmic reticulum-associated protein degradation of cystic fibrosis transmembrane conductance regulator in yeast. Mol Biol Cell 12, 1303–1314.
Zhao Y, Macgurn JA, Liu M, Emr S (2013). The ART-Rsp5 ubiquitin ligase network comprises a plasma membrane quality control system that protects yeast cells from proteotoxic stress. Elife 2, e00459.